ORIGINAL

B. Premachandran · C. Balaji

Mixed convection heat transfer from a horizontal channel with protruding heat sources

Abstract A numerical investigation is carried out to study fluid flow and heat transfer characteristics of conjugate mixed convection from a two dimensional horizontal channel with four protruding heat sources mounted on one of the finite thick channel walls. The flow is assumed as laminar, hydrodynamically and thermally developing. Water and FC70 are the fluids under consideration. The geometric parameters such as spacing between the channel walls (S), size of protruding heat sources ($L_h \times t_h$), thickness of substrate (t) and spacing between heat sources (b) are fixed. Results are presented to show the effect of parameters such as Re_S, Gr_S^*, Pr, k_p/k_f and k_s/k_f on fluid flow and heat transfer characteristics. Using the method of asymptotic expansions, correlations are also presented for the maximum temperature of heat source.

List of symbols

A	Aspect ratio, L/S
b	Spacing between the heat sources, m
c	Specific heat, J/kg K
g	Acceleration due to gravity, 9.81 m/s^2
Gr_S^*	Modified Grashof number, based on volumetric heat generation, $g\beta \Delta T_{ref} S^3/v^2$
Gr	Grashof number defined with wall temperature, $g\beta(T_H-T_C)L_c^3/v^2$
k	Thermal conductivity, W/mK
L_h, t_h	Width and height of the protruding heat source, respectively, m
L_c, t_c	Height and thickness of the cavity wall, respectively, m
L	Length of the channel walls, m
Nu_{avg}	Average Nusselt number based on L_c, $\int_0^1 \mathrm{Nu}_Y \, dY$
Nu_Y	Local Nusselt number based on L_c, $-(\partial\theta/\partial X)_{X=0}$
p	Pressure at any location in the computational domain, Pa
P	Non-dimensional pressure at any location in the computational domain
Pe_S	Peclet number based on S, $u_\infty S/\alpha$
Pr	Prandtl number, v/α
q_v	Volumetric heat generation from the protruding heat sources, W/m^3
Re_S	Reynolds number based on S, $u_\infty S/v$
Ri_S^*	Modified Richardson number based on S, $(\mathrm{Gr}_S^*/\mathrm{Re}_S^2)$ or $(g\beta\Delta T_{ref}S/u_\infty^2)$
S	Spacing between the channel walls, m
t'	Time, s
t	Thickness of the plate, m
T	Temperature, K
u	Horizontal velocity, m/s
U	Non-dimensional horizontal velocity, u/u_∞
v	Vertical velocity, m/s
V	Non-dimensional vertical velocity, v/u_∞
x,y	Horizontal and vertical distances, respectively, m
X, Y	Non-dimensional horizontal and non-dimensional vertical distances, x/S, y/S, respectively

Greek symbols

α	Thermal diffusivity of the fluid, m^2/s
β	Isobaric cubic expansivity of the fluid, $-1/\rho(\partial\rho/\partial T)_P$, 1/K
δ	Convergence criterion, in fractional form, $|(\phi_{new}-\phi_{old})/\phi_{new}|$
$\varepsilon_1,\varepsilon_2,\varepsilon_3,\varepsilon_4,\varepsilon_5$	Parameters in the asymptotic expansion
ϕ	Any variable (U, V or θ), over which convergence is being tested for
v	Kinematic viscosity of fluid, m^2/s

B. Premachandran · C. Balaji (✉)
Heat Transfer and Thermal Power Laboratory,
Department of Mechanical Engineering,
Indian Institute of Technology Madras,
Chennai, 600 036, India
E-mail: balaji@iitm.ac.in
Fax: +91-44-2350509

θ	Non-dimensional temperature at any location in the computational domain, $(T-T_\infty)/\Delta T_{ref}$ or $(T-T_C)/\Delta T_{ref}$
ρ	Density of the fluid, kg/m^3
τ	Non-dimensional time, $u_\infty t'/S$
ψ	Non-dimensional stream function, $U=\partial\psi/\partial Y$, $V=-\partial\psi/\partial X$

Subscripts

c	Cavity
C	Cold
f	Fluid
h	Heat source
H	Hot
max	Maximum
new, old	Values of the dependent variables (U, V, θ) obtained from the present and previous iterations
p	Protruding heat source
ref	Reference value
s	Substrate
∞	Ambient

Miscellaneous symbol

| ΔT_{ref} | Reference temperature difference, $(q_v L_h t_h/k_f)$ or (T_H-T_C), K |

1 Introduction

Free, forced or mixed convection air-cooling of electronic components is inexpensive and simple to design. However, if the heat flux from the electronic component is very high, liquid cooling is preferred because of high heat transfer coefficients associated with them.

Most of the literature available, on cooling of electronic components, focus on forced convection or mixed convection air-cooling. Davalath and Bayazitolgu [1] presented results of a numerical study of conjugate forced convection air-cooling of three protruding heat sources. A fully developed velocity profile was specified at the inlet of the channel. Two cases, namely adiabatic walls and conducting finite thick walls were considered as substrate to study the effect of conduction in substrate. The effects of Reynolds number on fluid flow and heat transfer were analyzed and results were also presented on the effect of Prandtl number. Kim and Anand [2] carried out a numerical investigation of forced convection conjugate heat transfer from protruding heat sources considering a uniform velocity profile at the inlet. A periodic boundary condition was used at the outer surface of the substrates to simulate a large number of circuit boards arranged in traverse direction. Young and Vafai [3] carried out a numerical analysis of conjugate forced convection air-cooling of heat generating

obstacles for a wide range of Re and conductivity ratio, k_p/k_f. The effects of geometric parameters were also studied extensively. Very recently, Furukawa and Yang [4] carried out a numerical study of forced convection conjugate heat transfer from protruding heat sources with air as the cooling medium. The effects of substrate conductivity and air gap between electronic chip and substrate on the heat transfer characteristics were also presented.

Brateen and Patankar [5] presented numerical results for hydrodynamically and thermally periodically developed mixed convection heat transfer from an isothermal protruding heat source mounted on either the top or bottom of the channel walls. Kim et al. [6] carried out a numerical study of fluid flow and heat transfer characteristics of mixed convection in a channel with protruding heat sources mounted on the bottom channel wall. Heindel et al. [7] carried out an experimental investigation of liquid cooling of heat generating rib for free convection dominant flow, mixed convection and forced convection heat transfer. Mahaney et al. [8] carried out numerical experiments on mixed convection from 4×3 chips flush mounted in a horizontal channel for $200 \leq Re \leq 4{,}000$ and $0.7 \leq Pr \leq 30$. Sathe and Joshi [9] presented numerical results of free convection liquid cooling from a heat source mounted on a substrate located in an enclosure for $10 \leq Pr \leq 1{,}000$ and $10^3 \leq Ra \leq 10^6$. Studies on mixed convection heat transfer for hydrodynamically and thermally developing flow in a channel with protruding heat sources mounted on a finite thick substrate to simulate liquid cooling of electronic chips are scarce. Hence, in this paper, a numerical investigation of conjugate mixed convection heat transfer from volumetrically heat generating rectangular components mounted on a finite thick channel wall has been carried out for water and FC70. The effects of Re_S, $Gr_S{}^*$, Pr, k_p/k_f and k_s/k_f on the heat transfer and fluid flow characteristics are presented.

The number of parameters that influence the heat transfer and fluid flow characteristics is, hence, large and a full scale parametric study with a view to develop a correlation for maximum temperature of the chip is extremely time consuming. However, a correlation for the maximum temperature will be extremely useful from an engineering standpoint. In view of the conflicting requirements, we can take recourse to the method of asymptotic expansion in our quest for a correlation. Balaji and Herwig [12] used an asymptotic approach [10, 11] for a problem that involves multimode heat transfer, natural convection with surface radiation from two-dimensional cavity with its top end open. They showed that the correlation arrived at by this asymptotic approach using a limited parametric study agrees well within $\pm 6\%$ with that based on curve fitting using multiple regression with a large number of data. Hence, in this study we use the above-mentioned asymptotic expansion to develop a correlation for the maximum temperature.

2 Mathematical model and method of solution

The geometry for the problem under consideration is shown in Fig. 1. The flow is assumed to be laminar, incompressible, hydrodynamically and thermally developing. The medium is assumed to have constant properties, outside of density, for which Boussinesq approximation is assumed to hold good. A psuedo-transient approach is used to obtain steady state solutions. In view of this, the governing equations are given in the time-dependent form as follows:

2.1 Equations for fluid side

Based on the above-mentioned assumptions, the non-dimensional form of the governing equations for fluid side can be written as

$$\frac{\partial U}{\partial X} + \frac{\partial V}{\partial Y} = 0 \tag{1}$$

$$\frac{\partial U}{\partial \tau} + U\frac{\partial U}{\partial X} + V\frac{\partial U}{\partial Y} = -\frac{\partial P}{\partial X} + \frac{1}{\mathrm{Re}_S}\left(\frac{\partial^2 U}{\partial X^2} + \frac{\partial^2 U}{\partial Y^2}\right) \tag{2}$$

$$\begin{aligned}\frac{\partial V}{\partial \tau} + U\frac{\partial V}{\partial X} + V\frac{\partial V}{\partial Y} &= -\frac{\partial P}{\partial Y} + \frac{1}{\mathrm{Re}_S}\left(\frac{\partial^2 V}{\partial X^2} + \frac{\partial^2 V}{\partial Y^2}\right) \\ &\quad + \frac{\mathrm{Gr}_S^*}{\mathrm{Re}_S^2}\theta\end{aligned} \tag{3}$$

$$\frac{\partial \theta}{\partial \tau} + U\frac{\partial \theta}{\partial X} + V\frac{\partial \theta}{\partial Y} = \frac{1}{\mathrm{Re}_S \mathrm{Pr}}\left(\frac{\partial^2 \theta}{\partial X^2} + \frac{\partial^2 \theta}{\partial Y^2}\right) \tag{4}$$

2.2 Equation for the solid region

Substrate

$$\mathrm{Pe}_S\left(\frac{\rho_s c_s}{\rho_f c_f}\right)\frac{\partial \theta}{\partial \tau} = \frac{k_s}{k_f}\left(\frac{\partial^2 \theta}{\partial X^2} + \frac{\partial^2 \theta}{\partial Y^2}\right) \tag{5}$$

Protruding heat sources

$$\mathrm{Pe}_S\left(\frac{\rho_p c_p}{\rho_f c_f}\right)\frac{\partial \theta}{\partial \tau} = \frac{k_p}{k_f}\left(\frac{\partial^2 \theta}{\partial X^2} + \frac{\partial^2 \theta}{\partial Y^2}\right) + \frac{S^2}{L_h t_h} \tag{6}$$

Equation 1 is the familiar continuity equation. Equations 2 and 3 are the X and Y momentum equations, respectively, and Eq. 4 is the equation of energy for the fluid region. Equations 5 and 6 are the energy equations for the substrate and protruding heat sources, respectively. The second term on the RHS of Eq. 6 is the source term that arises because of the volumetric heat generation.

2.3 Boundary conditions

Adiabatic boundary condition is imposed on the outer surfaces of the channel walls.

Inlet boundary conditions The fluid is assumed to enter the channel with uniform velocity and temperature profiles, and the appropriate boundary conditions are,

$$U = 1.0 \tag{7}$$

$$V = 0 \tag{8}$$

$$\theta = 0 \tag{9}$$

Outlet boundary conditions For the outlet of the computational domain, the following boundary conditions are used for any variable ϕ.

$$\frac{\partial^2 \phi}{\partial X^2} = 0 \tag{10}$$

For the top and bottom of the extended computational domain, the following boundary conditions are imposed

$$\frac{\partial U}{\partial Y} = 0 \tag{11}$$

Fig. 1 a Geometric configuration of the horizontal channel with protruding heat sources. **b** Computational domain with boundary conditions
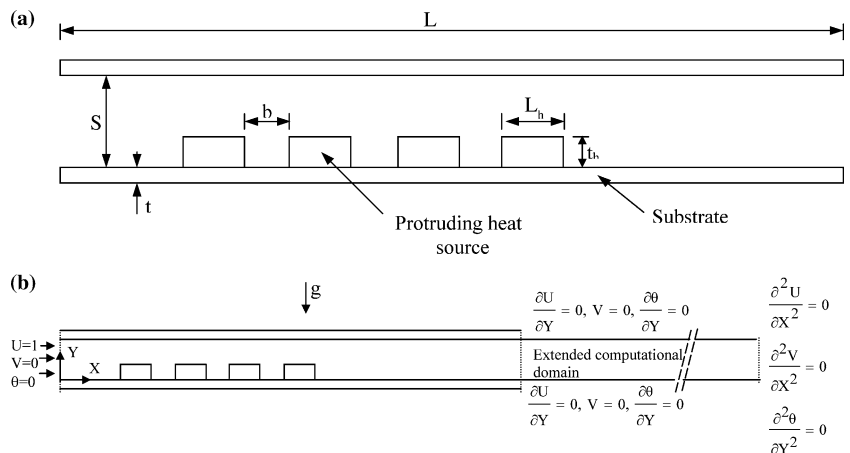
$$V = 0 \tag{12}$$

$$\frac{\partial \theta}{\partial Y} = 0 \tag{13}$$

3 Solution procedure

The governing equations are solved by a finite volume technique using SIMPLE algorithm [13]. A pseudo-transient explicit time marching approach is adopted to obtain steady state solutions. The code has been validated for mixed convection from an isothermal vertical channel by comparing the results obtained with those of Aung and Worku [14]. The outlet velocity and temperature profiles are compared for an aspect ratio of 4 and $Gr/Re = 250$. Figure 2a,b show that the results obtained by the present study compare well with those of Aung and Worku. To validate the code for the conjugate heat transfer problems, the results of the present study are compared with the numerical results of Kaminsky
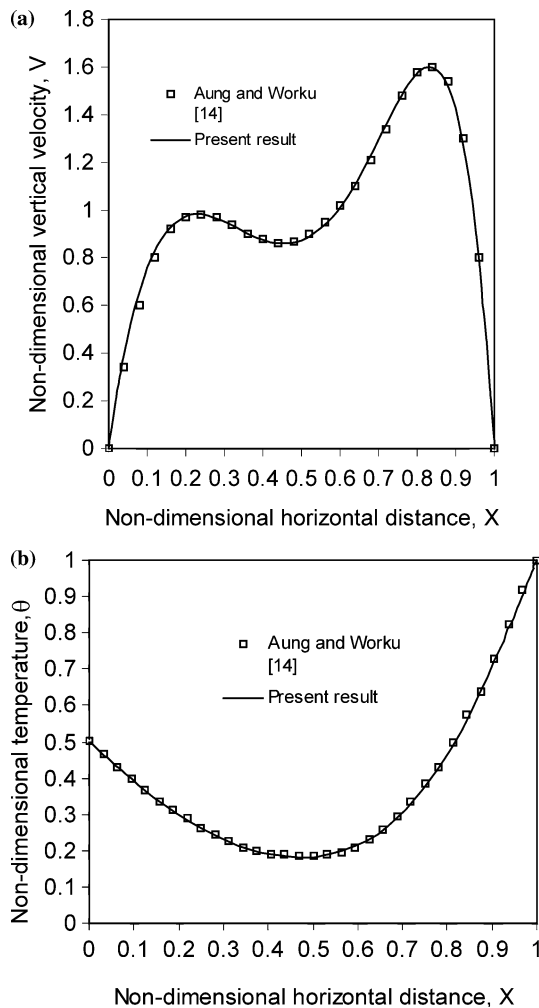
Table 1 Comparison of the average Nusselt number (Nu_{avg}) value for $t_c/L_c = 0.2$ obtained from present study with those of Kaminski and Prakash [15]

Gr	$k_s L_c / k_f t_c$	Kaminski and Prakash [15]	Present study
10^3	5	0.87	0.8742
	25	1.02	1.0282
	50	1.04	1.0514
10^5	5	2.08	2.0805
	25	3.42	3.4059
	50	3.72	3.7448
10^6	5	2.87	2.8482
	25	5.89	5.8385
	50	6.81	6.7448
5×10^6	5	3.35	3.3267
	25	8.07	7.9661
	50	9.86	9.7102
10^7	5	3.53	3.5108
	25	9.08	8.9561
	50	11.39	11.1978

and Prakash [15] for the case of conjugate natural convection in a square cavity with one finite thick wall. The average Nusselt number calculated for various wall conductivities and thicknesses by present code are shown in Table 1 and it can be seen that the results of the present study agree well with those of [15].

To ensure that the results obtained by the numerical study are independent of the computational grid, a grid independence study has been carried out. Based on this grid independence study, it is seen that 22,460 nodal points are necessary and sufficient and hence all subsequent calculations are based on 22,460 nodal points. Details of the grid independence study are presented in Table 2. A convergence criterion δ, of 1×10^{-5} has been imposed on all the three variables U, V and θ.

4 Result and discussion

Results have been obtained for a wide range of Re_S, Pr, Gr_S^*, k_p/k_f and k_s/k_f. For the present study, water and FC70 are considered as the coolants. Thermo physical properties of FC70 at 25°C are as follows: $\rho = 1,940$ kg/m^3, $\nu = 14 \times 10^{-6}$ m^2/s, $k_f = 0.07$ W/mK, $\beta = 0.001$ K^{-1}, $c_p = 1.0467$ kJ/kg K. The geometric parameters selected for present study are as follows: $S = 25 \times 10^{-3}$ m, $t = 2.5 \times 10^{-3}$ m, $b = 10 \times 10^{-3}$ m, $L_h = 15 \times 10^{-3}$ m, $t_h = 7.5 \times 10^{-3}$ m and $L = 300 \times 10^{-3}$ m. The parameters used in the present study are given in Table 3. The substrate is made up of a combination of epoxy-

Fig. 2 Comparison of the velocity and temperature profiles at the channel exit obtained in the present study with available results

Table 2 Grid independence study analysis in the present study ($Re_S = 500$, Pr = 6.15, $k_p/k_f = 10.32$, $k_s/k_f = 0.98$)

No. of nodal points	θ_{max}	Percentage change
16,730	0.07	–
22,460	0.0776	9.79
34,600	0.0782	0.76

Table 3 Parameter values used in present study ($T_\infty = 25$°C)

Parameter	Range	Units
Re	200–1,000	–
Pr	6.15–406.12	–
Gr_S^*	9.09×10^6–2.7×10^7	–
q_v	5×10^5–3×10^6	W/m^3
k_f	0.07, 0.61	W/mK
k_s	0.6–30	W/mK
k_p	0.63–63	W/mK

glass, copper, or ceramic laminates with an effective thermal conductivity, k_s of 0.6 W/mK [9]. Hence $k_s = 0.6$ W/mK is taken as the reference value.

Fig. 3 Effect of Re_S on flow pattern for Pr = 6.15 **a** Streamline plot for $Re_S = 200$, and $Ri_S^* = 227.4$ **b** enlarged views of flow patterns in cavities for $Re_S = 200$ and $Ri_S^* = 227.4$ and **c** enlarged views of flow patterns in cavities for $Re_S = 1,000$ and $Ri_S^* = 9.09$

4.1 Effect of Reynolds number, Re_S

Figure 3a shows the streamline pattern (contours of non-dimensional stream function, ψ) for $Re_S = 200$, Pr = 6.15 and $Ri_S^* = 227.4$. Figure 3b, c show the flow field in three cavities, formed by protruding heat sources, for the case of $Re_S = 200$ and 1,000, respectively. It is seen that buoyancy effect dominates in the cavity flows for $Re_S = 200$. At this Reynolds number, two circulation loops are formed (Fig. 3b). The end faces of the protruding heat sources and the top surface of substrate act as left and right facing L corners with a heated vertical plate. The effect of buoyancy is also observed beyond the last heat source. For the case of $Re_S = 1,000$, the effect of buoyancy on the flow pattern is negligible as expected and the fluid in the cavity is predominantly driven by the mainstream flow as can be seen in Fig. 3c. The effect of buoyancy on the flow pattern is also negligible for the case of FC70 for $200 \leq Re_S \leq 1,000$.
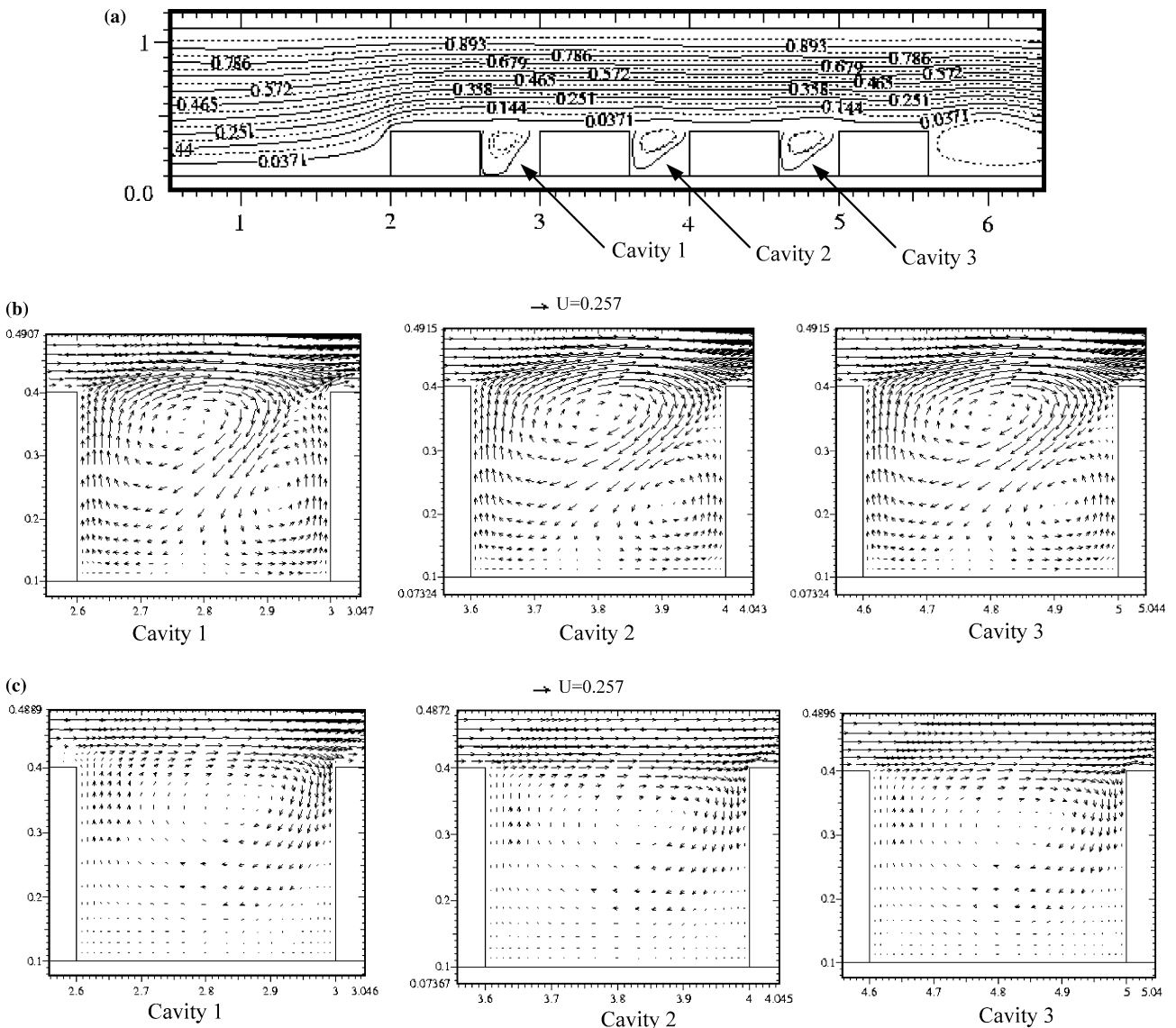
Fig. 4 Effect of buoyancy on flow pattern for Pr = 6.15 **a** isotherm plot for Re = 200, and $Ri_S{}^* = 227.4$ **b** isotherm plot for Re = 1,000 and $Ri_S{}^* = 9.09$
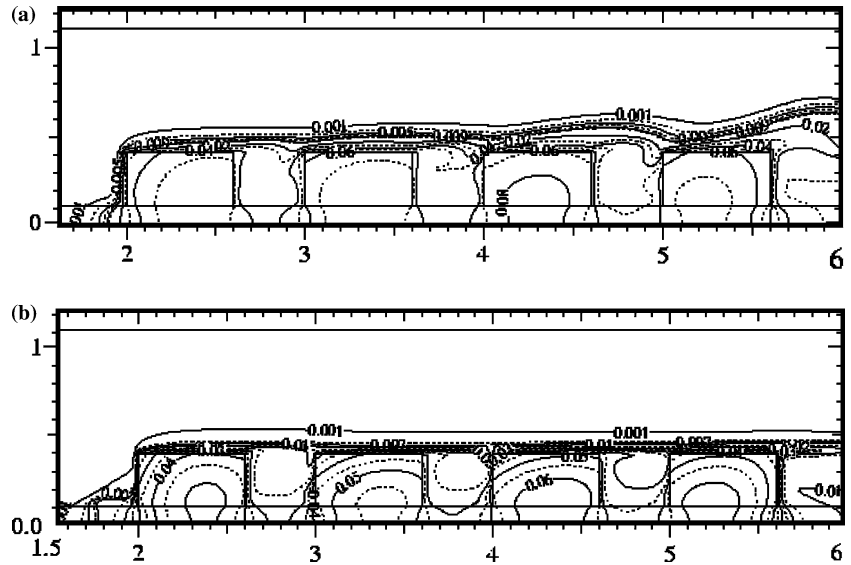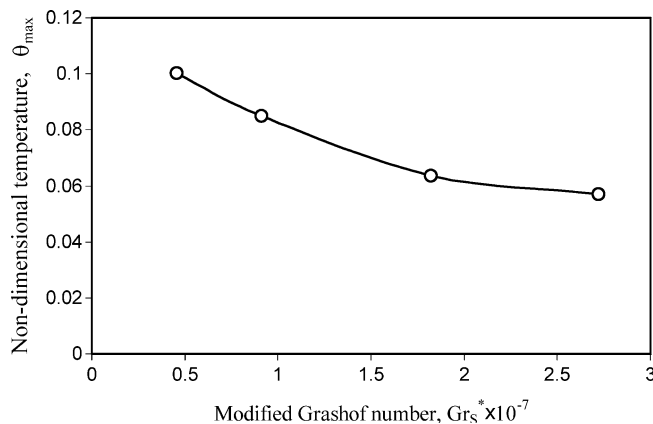

Figure 4a, b show the isotherms for the two values of Re_S, 200 and 1,000 for Pr = 6.15. The circulation after the last protruding heat source has much more contact with the mainstream flow and hence the cooling of last chip is better than the penultimate chip and hence the maximum temperature of the last heat source is less than that of the penultimate chip.

4.2 Effect of modified Grashof number, $Gr_S{}^*$

The effect of modified Grashof number, $Gr_S{}^*$ on the maximum temperature is presented for $Re_S = 200$ and Pr = 6.15. To study the effect of $Gr_S{}^*$, the values of q_v considered are 5×10^5, 1×10^6, 2×10^6 and 3×10^6. Figure 5 shows that the non-dimensional maximum temperature decreases non-linearly (dimensional maximum temperature increases) as $Gr_S{}^*$ increases.

4.3 Effect of ratio of thermal conductivities of protruding heat source to fluid, k_p/k_f

Isotherms for two thermal conductivity values, 0.63 and 63 W/mK for $Re_S = 100$ and Pr = 6.15 are shown in Fig. 6a, b. Figure 6c shows the change in temperature distribution at the top surface of substrate. As the thermal conductivity of protruding heat source increases, the maximum temperature decreases, as expected. The non-dimensional maximum temperature increases sharply when k_p/k_f decreases from 10.32 to 1.032 compared to the change in non-dimensional maximum temperature when k_p/k_f decreases from 103.2 to 10.32 (Fig. 6d). The maximum temperature of the heat source for thermal conductivities 0.63, 6.3 and 63 W/mK are 331, 313.7 and 306 K, respectively.

4.4 Effect of ratio of thermal conductivities of substrate to fluid, k_s/k_f

Figure 7 shows the variation of non-dimensional maximum temperature with k_s/k_f. As k_s/k_f increases the non-dimensional maximum temperature decreases mildly and nonlinearly and there is no drastic change in the maximum temperature unlike what was observed changing for k_p/k_f.

4.5 Effect of Prandtl number, Pr

Figure 8 shows the effect of Pr on the maximum temperature of heat source for various Re_S values for $q_v = 1 \times 10^6$ W/m^3, $k_s = 0.6$ W/mK and $k_p = 6.3$ W/mK. For all values of Re_S, the maximum temperatures predicted for water are comparatively lower than that of FC70.

Fig. 5 Variation of non-dimensional maximum temperature with modified Grashof number $Gr_S{}^*$ for $Re_S = 200$

516

Fig. 6 Effect of thermal conductivity of heat source ($\mathrm{Re}_S = 100$, $\mathrm{Pr} = 6.15$). **a** $k_\mathrm{p}/k_\mathrm{f} = 0.63$ W/mK, **b** $k_\mathrm{p}/k_\mathrm{f} = 63$ W/mK, **c** temperature distribution at top surface of the substrate, **d** variation of non-dimensional maximum temperature with $k_\mathrm{p}/k_\mathrm{f}$
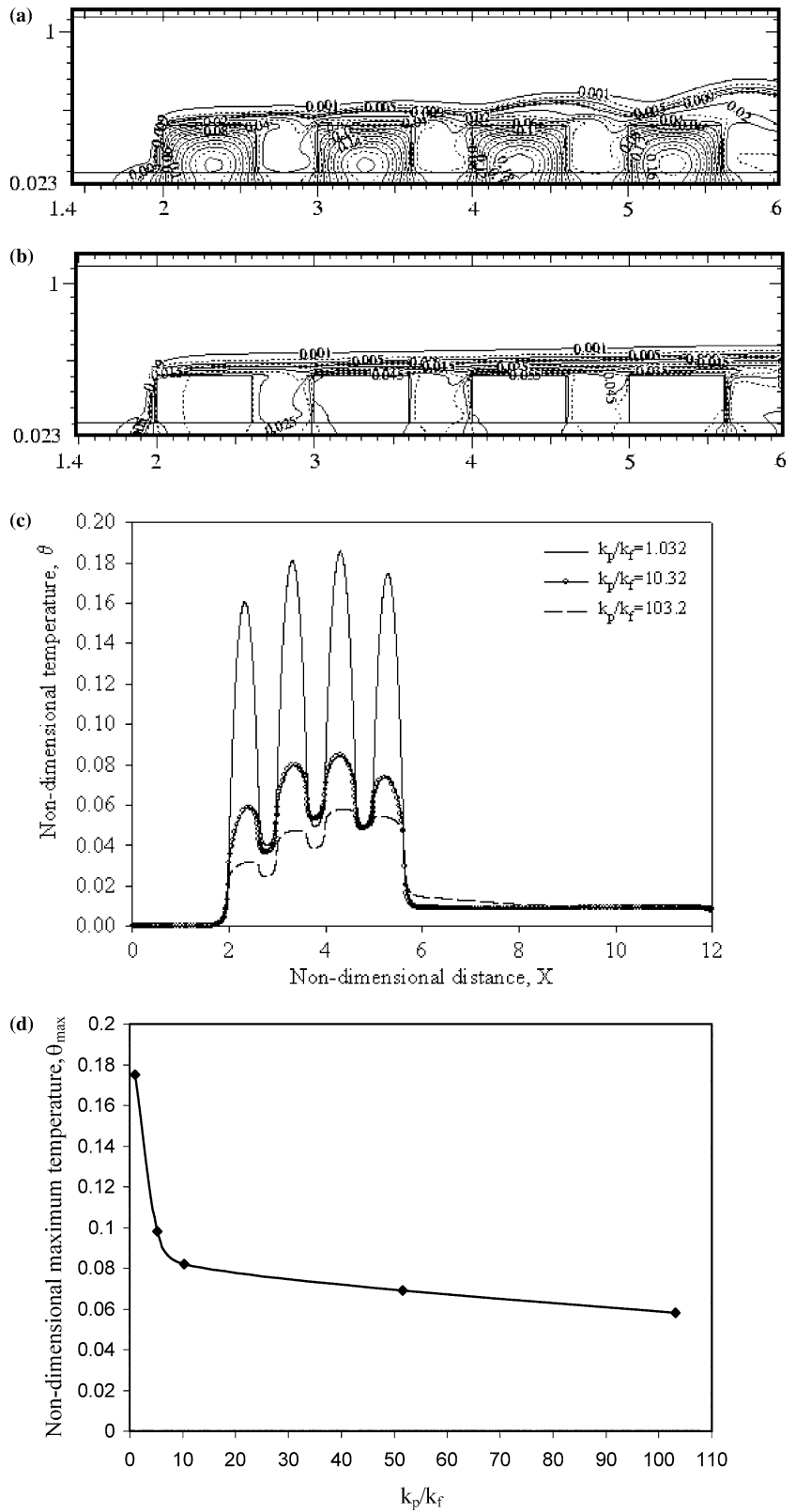
4.6 Effect of buoyancy

A parametric study was also carried out to quantify the effect of buoyancy by neglecting the buoyancy term from the y-momentum equation. A comparison of maximum temperatures obtained by considering buoyancy and that obtained by neglecting buoyancy is shown in a parity plot (Fig. 9) for $\mathrm{Re}_S = 200$–1,000. As
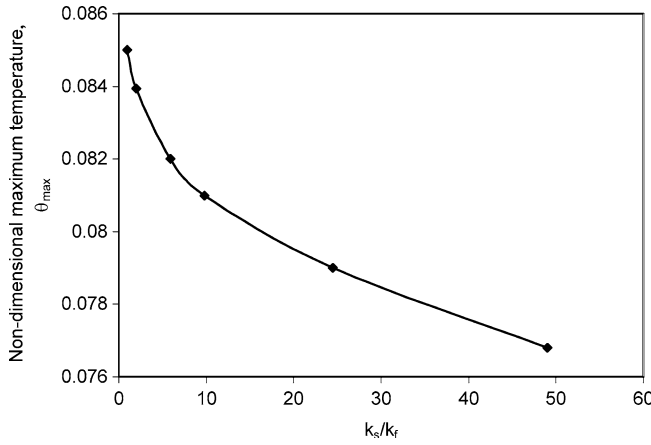
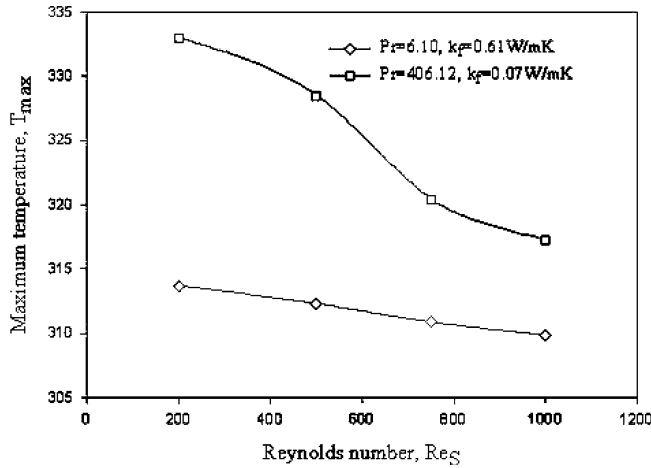**Fig. 7** Variation of non-dimensional maximum temperature with k_s/k_f

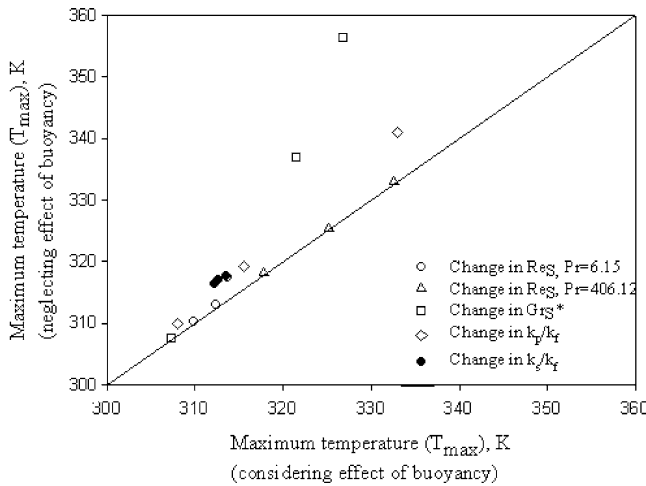**Fig. 8** Variation of maximum temperature with Re_S for two values of Pr

Fig. 9 Effect of buoyancy on the maximum temperature in the chip

expected, all the points are on one side of the parity line, conforming that buoyancy helps in the reduction of the maximum temperature in the chip. The legends in the plot succinctly bring out the effect of the individual parameters on the maximum temperature. For some cases, $Re_S = 200–1,000$ and $Pr = 406.12$, it is seen that "neglecting" buoyancy will not result in a significant error in the predictions.

4.7 Correlation for maximum temperature

One of the principal objectives in the design of the cooling system for electronic equipment is to reduce maximum temperature of the electronic components. Hence, a correlation for predicting the maximum temperature attained in the electronic chip is highly desirable. However, as already discussed, with a limited parametric study, a simple asymptotic expansion approach offers the best bet for obtaining a correlation for the maximum temperature.

Asymptotic expansion approach involves the expansion of the solution to the problem around a particular solution that is taken as the reference. A detailed procedure of this method is presented in [12]. The independent variables identified for the present study are Re_S, Gr_S^*, Pr, k_s/k_f, k_p/k_f. The reference values chosen for the expansion are $Re_S = 100$, $Pr = 6.15$, $Gr_S^* = 9{,}096{,}000$, $k_p/k_f = 10.32$, $k_s/k_f = 0.98$. The θ_{max} for this reference set of parameters, $\theta_{max,ref} = 0.085$. A preliminary analysis showed that linear expansion is sufficient for Re_S, Gr_S^*, Pr and k_s/k_f while quadratic expansion is used for k_p/k_f. θ_{max} can now be expanded in the vicinity of $\theta_{max, ref}$ as follows:

$$\theta_{max} = \theta_{max,ref} + \frac{\partial \theta_{max}}{\partial \varepsilon_1}\left(\varepsilon_{1,ref} - \varepsilon_1\right) + \frac{\partial \theta_{max}}{\partial \varepsilon_2}\left(\varepsilon_{2,ref} - \varepsilon_2\right)$$
$$+ \frac{\partial \theta_{max}}{\partial \varepsilon_3}\left(\varepsilon_{3,ref} - \varepsilon_3\right)$$
$$+ \frac{\partial \theta_{max}}{\partial \varepsilon_4}\left(\varepsilon_{4,ref} - \varepsilon_4\right) + \frac{1}{2}\frac{\partial^2 \theta_{max}}{\partial \varepsilon_4^2}\left(\varepsilon_{4,ref} - \varepsilon_4\right)^2$$
$$+ \frac{\partial \theta_{max}}{\partial \varepsilon_5}\left(\varepsilon_{5,ref} - \varepsilon_5\right) \tag{14}$$

where $\varepsilon_1 = (Re/Re_{ref})^{0.5}$, $\varepsilon_{1ref} = 1.0$; $\varepsilon_2 = (Pr/Pr_{ref})^{0.33}$, $\varepsilon_{2ref} = 1.0$; $\varepsilon_3 = (Gr_{S\ ref}^*)^{0.25}$, $\varepsilon_{3ref} = 1.0$; $\varepsilon_4 = ((k_p/k_f)/(k_p/k_f)_{ref})^{0.25}$, $\varepsilon_{4ref} = 1.0$; $\varepsilon_5 = ((k_s/k_f)/(k_s/k_f)_{ref})^{0.25}$, $\varepsilon_{5ref} = 1.0$.

The non-dimensional maximum temperature changes sharply as k_p/k_f increased from 1.032 to 10.32 (Fig. 6d). Hence two ranges, $1.032 \leq k_p/k_f \leq 10.32$ and $10.32 \leq k_p/k_f \leq 103.2$ are considered in the calculation of $\partial \theta_{max}/\partial \varepsilon_4$. The coefficients of Eq. 14, $\partial \theta_{max}/\partial \theta_1$, $\partial \theta_{max}/\partial \varepsilon_2$, $\partial \theta_{max}/\partial \varepsilon_3$, $\partial \theta_{max}/\partial \varepsilon_4$ and $\partial \theta_{max}/\partial \varepsilon_5$, are evaluated one at a time by obtaining solutions to the original governing equation with all but one parameter fixed at the reference values. For example, to evaluate $\partial \theta_{max}/\partial \varepsilon_1$, a solution is obtained for $\varepsilon_1 \neq 1$ while ε_2 to ε_5 are maintained at the reference value of 1. From Eq. 14

Table 4 Range of parameters considered for the correlations

$200 \leq \mathrm{Re}_S \leq 1{,}000$
$6.15 \leq \mathrm{Pr} \leq 40$
$9.09{\times}10^6 \leq \mathrm{Gr}_S^* \leq 2.7{\times}10^7$
$1.032 \leq k_{\mathrm{p}}/k_{\mathrm{f}} \leq 103.2$
$0.98 \leq k_{\mathrm{s}}/k_{\mathrm{f}} \leq 49.0$

it is clear that for determining $\partial\theta_{\max}/\partial\varepsilon_1$, Re_S alone needs to be changed. Following a similar procedure, other coefficients can be evaluated. Substituting these into Eq. 14 we now obtain correlations for $\theta_{\max}$ and these turn out to be:

1. For $10.32 \leq (k_{\mathrm{p}}/k_{\mathrm{f}}) \leq 103.2$

$$
\begin{aligned}
\theta_{\max} = {} & \theta_{\max,\mathrm{ref}} + 0.01268(1 - \varepsilon_1) + 0.04512(1 - \varepsilon_2) \\
& + 0.1162(1 - \varepsilon_3) + 0.0278(1 - \varepsilon_4) \\
& - 0.0080(1 - \varepsilon_4)^2 + 0.0056(1 - \varepsilon_5)
\end{aligned} \tag{15}
$$

2. For $1.032 \leq (k_{\mathrm{p}}/k_{\mathrm{f}}) \leq 10.32$

$$
\begin{aligned}
\theta_{\max} = {} & \theta_{\max,\mathrm{ref}} + 0.01268(1 - \varepsilon_1) + 0.04512(1 - \varepsilon_2) \\
& + 0.1162(1 - \varepsilon_3) + 0.0135(1 - \varepsilon_4) \\
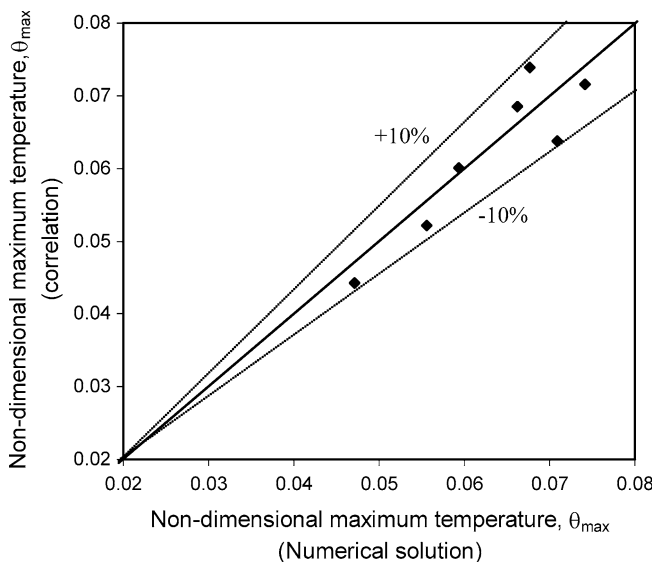& - 0.0491(1 - \varepsilon_4)^2 + 0.0056(1 - \varepsilon_5)
\end{aligned} \tag{16}
$$

Equations 15 and 16 are valid for the range of parameters given in Table 4. A Parity plot (Fig. 10) shows that the maximum temperature, $\theta_{\max}$ obtained from the numerical solutions and $\theta_{\max}$ obtained from the above correlations compare very well.

4.8 Conclusions

Results of a numerical study of conjugate mixed convection liquid cooling from a horizontal channel with volumetric heat generating protruding heat sources have been presented in this paper. The effect of Re_S, Pr, thermal conductivity of protruding heat source, and the thermal conductivity of substrate have been analyzed. The main conclusions of the study are:

1. The effect of buoyancy is significant for a fluid like water, while it is negligible for FC70.
2. The thermal conductivity of the protruding heat source affects the maximum temperature to the extent of 40% when $k_{\mathrm{p}}/k_{\mathrm{f}}$ varies from 1.032 to 10.32, for water when $\mathrm{Re}_S = 200$ and $q_{\mathrm{v}} = 1 \times 10^6$ W/m^3.
3. Buoyancy can reduce the maximum temperature by as much as 35% for water when $\mathrm{Re}_S = 200$ and $q_{\mathrm{v}} = 3 \times 10^6$ W/m^3.
4. Even with a limited parametric study, a correlation for maximum temperature based on asymptotic expansion gives reasonably accurate predictions.

Fig. 10 Parity plot showing agreement of $\theta_{\max}$ (correlation) with $\theta_{\max}$ (data)

References

1. Davalath J, Bayazitoglu Y (1987) Forced convection cooling across rectangular blocks. ASME J Heat Transfer 109:321–328
2. Kim SH, Anand AK (1994) Laminar developing flow and heat transfer between a series of parallel plates with surface mounted discrete heat sources. Int J Heat Mass Transfer 37:2231–2244
3. Young TM, Vafai K (1998) Convective flow and heat transfer in a channel containing multiple heated obstacles. Int J Heat Mass Transfer 41:3279–3298
4. Furukawa T, Yang W (2003) Thermal-fluid flow in parallel boards with heat generating blocks. Int J Heat Mass Transfer 46:5005–5015
5. Brateen EM, Patankar SV (1985) Analysis of laminar mixed convection in shrouded array of heated rectangular blocks. Int J Heat Mass Transfer 28:1699–1709
6. Kim SY, Sung HJ, Hyun JM (1992) Mixed convection from multi-layered boards with cross-stream wise periodic boundary conditions. Int J Heat Mass Transfer 35:2941–2952
7. Heindel TF, Incropera FP, Ramadhyani R (1992) Liquid immersion cooling of longitudinal array of discrete heat sources in protruding substrates: 1. Single phase forced convection. J Electronic Packaging 114:55–62
8. Mahaney HV, Incropera FP, Ramadhyani S (1990) Comparison of predicted and measured convection heat transfer from an array of discrete sources in a horizontal rectangular channel. Int J Heat Mass Transfer 33:1233–1245
9. Sathe SB, Joshi Y (1992) Natural convection liquid cooling of a substrate-mounted protrusion in a square enclosure: a parametric study. ASME J Heat Transfer 114:401–409
10. Herwig H (1985) Effect of variable properties on momentum and heat transfer in a tube with constant heat flux across the wall. Int J Heat Mass Transfer 28:424–431
11. Herwig H, Voigt M, Bauhaus FJ (1989) The effect of variable properties on momentum and heat transfer in a tube with constant wall temperature. Int J Heat Mass Transfer 32:1907–1915
12. Balaji C, Herwig H (2003) The use of ACFD approach in problems involving surface radiation and free convection. Int Commun Heat Mass Transfer 30:251–259
13. Patankar SV (1980) Numerical heat transfer and fluid flow. Hemispere, New York
14. Aung W, Worku G (1986) Developing flow and flow reversal in a vertical channel with asymmetric wall temperatures. ASME J Heat Transfer 108:299–304
15. Kaminski DA, Prakash C (1986) Conjugate natural convection in a square enclosure: effect of conduction in one of the vertical walls. Int J Heat Mass Transfer 29:1979–1988